



Effective Thermal Design Concept of Sabatier Reactor by Controlling Catalyst Distribution Profile

Shinya Sakamoto¹ · Tsuneyoshi Matsuoka¹ · Yuji Nakamura¹

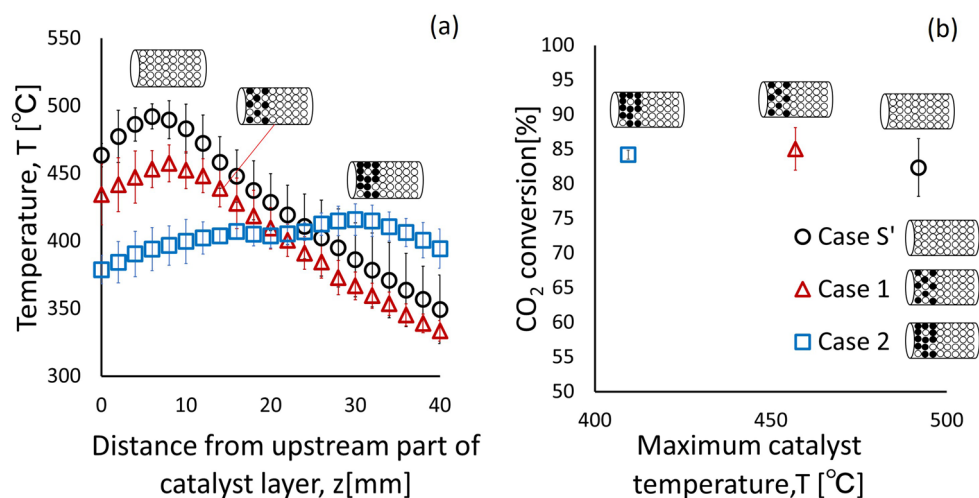
Received: 3 December 2019 / Accepted: 21 March 2020
 © Springer Science+Business Media, LLC, part of Springer Nature 2020

Abstract

This study presents the effective thermal design concept of exothermic Sabatier reactor, which shall convert carbon dioxide with hydrogen to produce water and methane (so-called “methanation”) assisted by the catalytic activity. Pellet type of Ru-based catalyst is packed in the preheated reactor tube and stoichiometric reactant gas mixture (CO₂ and H₂) flows at the prescribed flow rate. By employing the present system, steady 1-D reaction field is successfully achieved. Bundled thermocouples are inserted from the downstream through the sealed yet movable connectors to obtain the steady-state temperature profile in the reactor. End gas is analyzed by gas chromatography to check the conversion performance. The following two series of reactor are tested; it has (1) uniform or (2) stepwise catalyst distribution. By using uniform catalyst bed, relatively strong peak in the temperature profile is appeared at the inlet and thermal damage of catalyst is highly expected to lose the durability. No significant improvement on reduction of the peak as well as the conversion performance even when the shorter heating regime is employed, although the peak location moves to downstream. Adopting the non-uniform (stepwise) catalyst distribution are effectively modifying the thermal structure in the reactor having the less-peak in the temperature profile without losing the conversion performance. Our study reveals the control of catalyst distribution is simple yet effective approach to achieve the uniform temperature profile even in 1-D flow reactor design at high conversion performance.

Graphic Abstract

The reactor temperature profile was achieved to be uniform by adopting stepwise catalyst distribution to prevent hot spots in the Sabatier reactor.



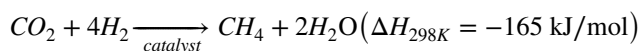
Keywords Sabatier reaction · Thermal control · Stepwise catalyst distribution

Extended author information available on the last page of the article

Published online: 01 April 2020

1 Introduction

Sabatier reaction is known as “methanation” to produce methane from carbon dioxide reacting with hydrogen. Water is also produced as bi-product. As shown in below, this is exothermic reaction accelerated over catalyst (Ru, Ni, Co, Fe) [1–4].



Recently this reaction has been paid attention in terms of carbon-recycle point of view; this enables us to reform the industrial product (CO_2) to the fuel (CH_4) [5, 6]. Although the need of excess hydrogen sounds quite unrealistic and there is no application to be employed, it is attractive for “unfamiliar” special environment; for instant in space.

Imagine that the highly sealed spacecraft cabin, we need high-level of material recycling with dependable system. Through the human activity, continuous oxygen supply as well as the removal of carbon dioxide (CO_2) is really indispensable [7], especially, establishment of the solid technology is highly demanded because the term of future manned space mission (e.g., go to Moon and Mars) become quite longer [8, 9]. At present, a removal of CO_2 has been achieved by the disposal filter, thus, large stock of filters are necessary [10]. Similarly oxygen is obtained through electrolysis of water (H_2O) so that large amount of water must be carried with us. Because the launching the heavy weight is the last issue for any space mission, even it is costly, less-weight system is highly demanded. Therefore, especially for space use, a novel technology to “convert” CO_2 to other chemical compound and recycling the water is recognized as the very important task. For this purpose, Sabatier reactor is attracted as the key technique and play important function on the closed-loop air revitalization (Fig. 1) [10, 11]. As learned from the figure, water is recycled and CO_2 is converted to CH_4 . Using high-temperature pyrolysis reactor, CH_4 can be converted to (solid) carbon and hydrogen ($\text{CH}_4 \Rightarrow \text{C(s)} + 2\text{H}_2$), additional H_2 can be recycled into the Sabatier system [12]. Ideally, no additional H_2O supply is needed and perfect material recycling system is achieved.

Currently major space agencies are positive to apply this system for future space mission [13, 14].

Although this technology sounds promising, there are severe engineering problems when practical use is considered. An overheating of the reactor (catalyst) is the one of most serious dangers triggered by the exothermic feature of the present system. Figure 2 shows the schematic illustration of the typical temperature dependency on CO_2 conversion performance over the typical catalyst. As shown in this figure, too-low temperature does not give any conversion but too-high temperature ($> 550^\circ\text{C}$) is also not good to bring the thermal damage (e.g. sintering) to the catalyst to destruct the catalytic activity for nickel-based catalyst [15]; according to the past work, due to atom migration sintering mechanism over 600°C , active surface area of nickel is decreased and catalytic activity per unit surface area becomes weakened. Even the other type of catalyst is used, the reaction path to CO formation shall be promoted over 420°C [16], which lead the reduction of conversion performance. In this sense, it is mandatory to manage the temperature in the reaction system well within certain range in order to work the scenario as expected. Recall that Sabatier reaction has the exothermic feature, it is understood that the careful thermal management to maintain the reaction in the preferred range is the key issue.

Suppose the reactor works in homogeneous system, it is not very difficult to manage the reaction temperature by controlling the temperature of the thermal bath surrounded over the reactor. However, most of practical reactor works as

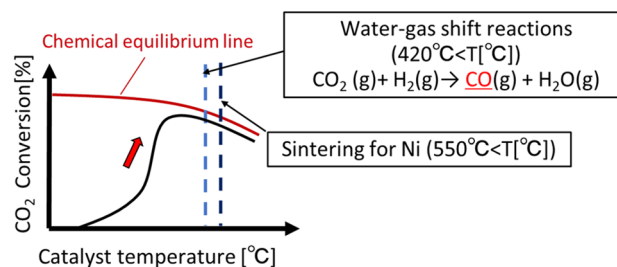
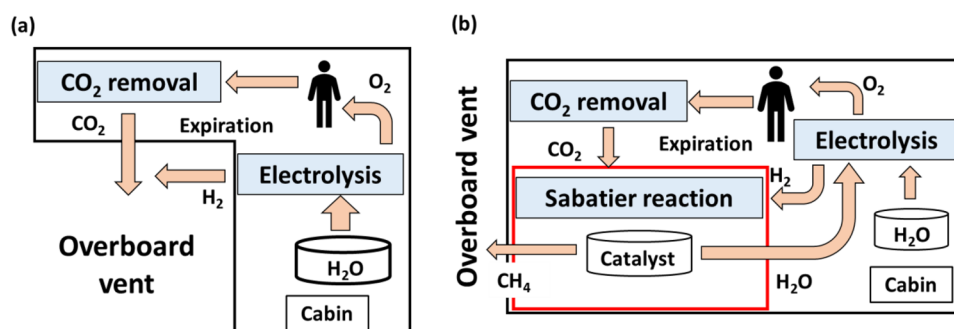


Fig. 2 Temperature dependency on the overall conversion of CO_2

Fig. 1 Air revitalization system a without sabatier assembly, b with sabatier assembly



inhomogeneous system; for instance, the common tube-type reactor system tends to have 1-D temperature profile along the flowing direction [17]. The relatively highly-reactive zone tends to appear in upstream resulting in appearance of sharp peak of the temperature there. Consequently, even the average temperature of the reactor is in the preferred range as discussed, the part of the reactor (catalyst) may be out of range to lead inevitable problems such as thermal damage of the local catalyst, CO production and the less conversion performance. In the worst case, thermal runaway may occur to completely damage the system to lose the stability. To improve the durability and stability under 1-D reaction system, effective thermal management concept must be introduced.

To date, several attempts with liquid and air cooling have been made to suppress the inhomogeneity of the temperature profile in the tube-type reactor [11, 18, 19]. Sun et.al have introduced the cooling system at the catalyst layer and successfully suppress the sharp temperature rise [19]. Although this attempt seems to work for scientific approach, having heating (to initiate) and cooling (to maintain) devices in the same reactor does sounds from engineering aspect.

In this work, for the better practical use of the Sabatier reactor, the lab-scaled test bench is developed and the capability of thermal management in small-scale test device is tested. The following two approaches are mainly considered for the present purpose; one is to apply the porous structure

to promote the heat recirculation toward the upstream and the other is to introduce stepwise catalyst distribution to control the heat release. Through the better control in both heat release and dissipation processes, we could seek the best thermal design to achieve the “nearly flat temperature profile” in the 1-D type reactor, which can provide durability as well as stability.

2 Experiment

2.1 Apparatus Overview

Figure 3 shows the schematic illustration of the reaction system developed in this study. CO₂ and H₂ (1/4 in volume ratio) are supplied into a gas mixer to form the reactant mixture, then air introduced into a reactor. Prior to loading the reactant gas, the reactor is preheated by the electric ribbon heater and kept at prescribing temperature (up to 250 °C) by adjusting the voltage applied into the heater. This preheating setting is kept unchanged (namely, heater is kept ON) during the test. When the system reaches the steady state, the product gas is collected at outlet the reactor by a Tedlar bag (sampling bag), and is analyzed by a gas chromatograph (Shimadzu Corporation GC-14B) with stainless column filled with Unibeads 1s (GL Science Inc).

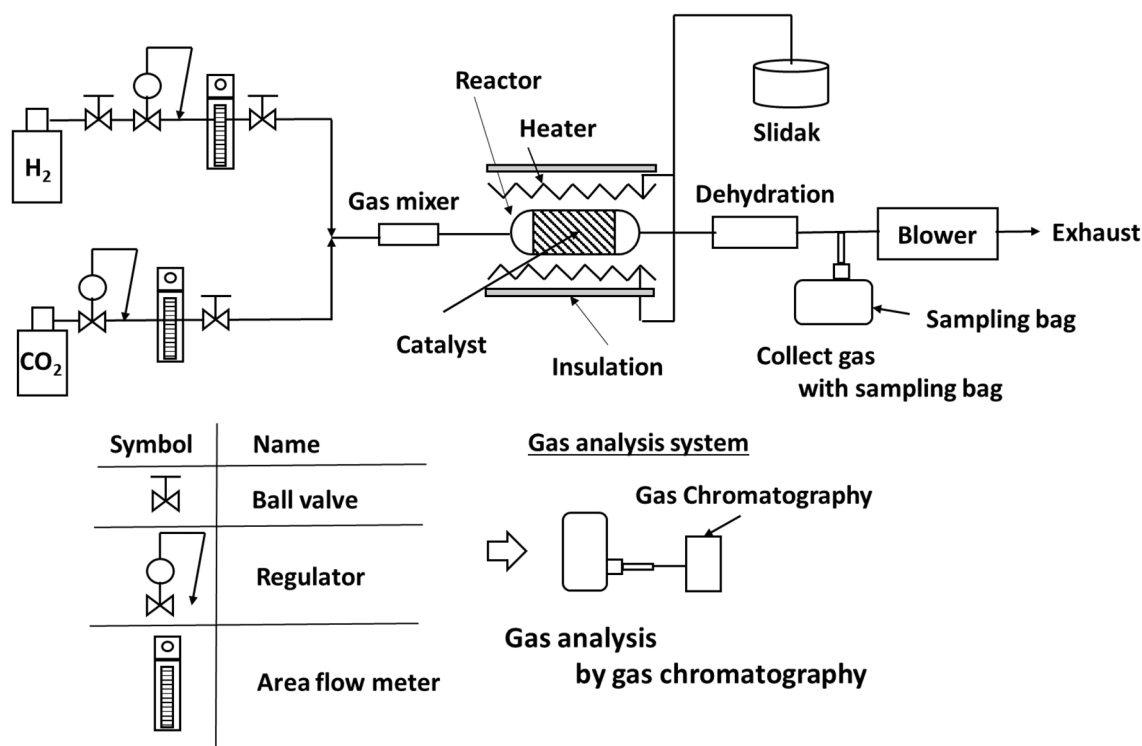


Fig. 3 Schematic illustration of the experimental apparatus of the presently-studied Sabatier reactor

The performance of the reactor is evaluated with the conversion ratio of CO_2 . The ratio is estimated by using the volume (mole) fraction of the unreacted CO_2 and produced CH_4 found in the product gas. In the present study, the CO_2 conversion rate (X_{CO_2}) is defined in the following Eq. (1).

$$X_{\text{CO}_2} = \frac{\text{Produced } \text{CH}_4}{\text{Produced } \text{CH}_4 + \text{unreacted } \text{CO}_2}, \quad (1)$$

Assuming that carbonate species in this system are mainly CH_4 and CO_2 , Eq. (1) give the representative conversion rate evaluated at outlet status. In reality, however, intermediate species (like CO) would be produced so that evaluation based on Eq. (1) may result in over-estimation. The applicability of this approach is confirmed through the gas analyses using two types of column (Rt-Msieve5A and Rt-Q-BOND) for typical case as shown in Fig. 4. Small amount of air is detected probably due to the remained air in the bag and they are eliminated in calculation of volume fraction of detected species. GC data revealed that the major carbonate species are CO , CO_2 and CH_4 and produced CO can be at most 2% in vol. when the peak temperature is 500 °C and even lower as the field temperature decreases (note that this

is the temperature range of concern in this study as shown in later). Therefore, selectivity to CH_4 formation is dominant under the condition studied in the present work and the above-mentioned assumption shall be acceptable.

2.2 Catalytic Reactor

Figure 5 shows the illustration of catalyst arrangement in the reactor. Reactor is made by aluminum tube and placed vertically with downward gas flow. The reactor is surrounded by a heater and thermal insulator to control the initial temperature of the reactor, as mentioned previously. Hereafter, the maintained temperature of the reactor wall is called “reactor temperature” throughout this study. Temperature inside the reactor is measured by thermocouples (denote TCs hereafter). Product gas is sampled at the end to be analyzed. The experiment is conducted by supplying H_2 and CO_2 at the flow rates of H_2 : 0.8 L/min and CO_2 : 0.2 L/min, respectively. Catalyst length (L , L_{mix}) applied in this study is varied by the adopted cases as summarized in Table 1, together with corresponding space velocities.

Catalyst used in this study is commercially available product (2 wt% $\text{Ru}/\text{Al}_2\text{O}_3$, N.E.CHEMCAT Corp.), which

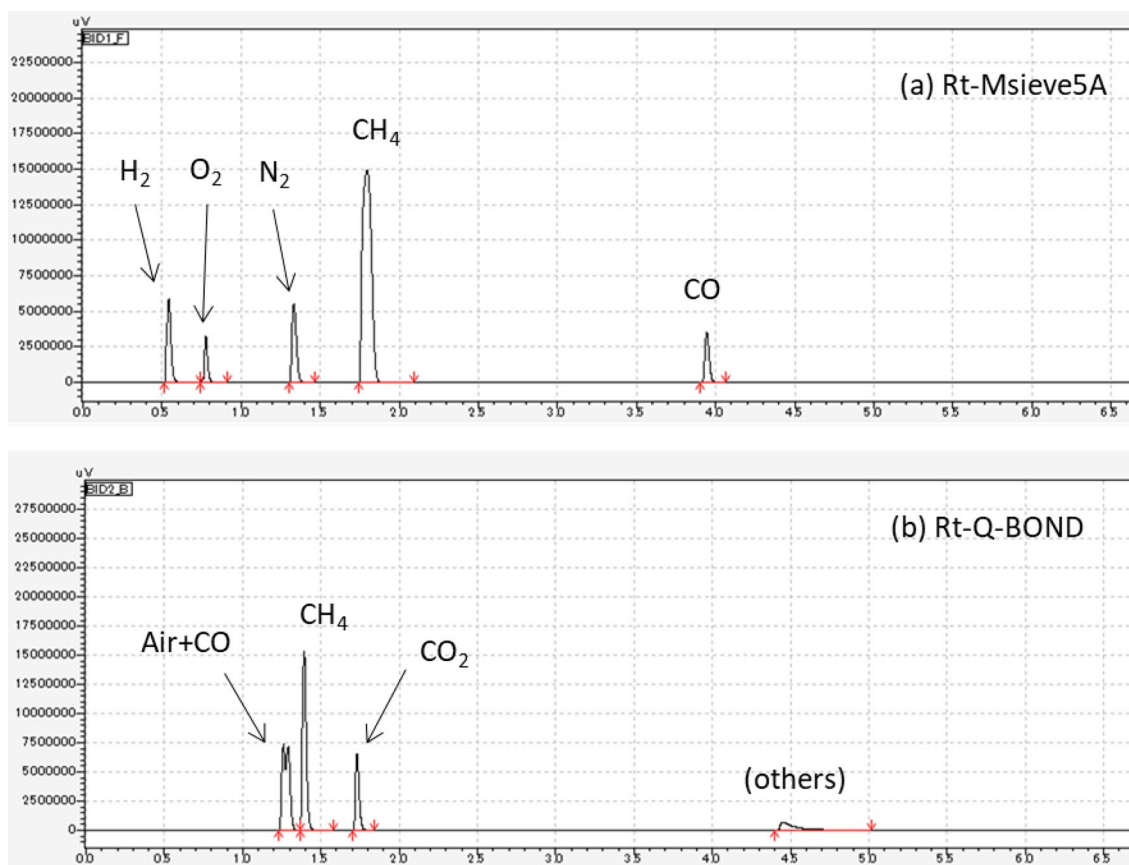


Fig. 4 Typical GC signal of end-gas analysis

Fig. 5 Tested reactor designs, **a** only catalyst is embedded and the heater covers the entire reactor, **b** only catalyst is embedded and the heater covers only the vicinity of the catalyst layer, **c** mixed-layer of catalyst and (chemically-inert) ceramic beads is placed in upstream (mixing ratio is varied: see Table 1) and the heater coverage area is the same as (b)

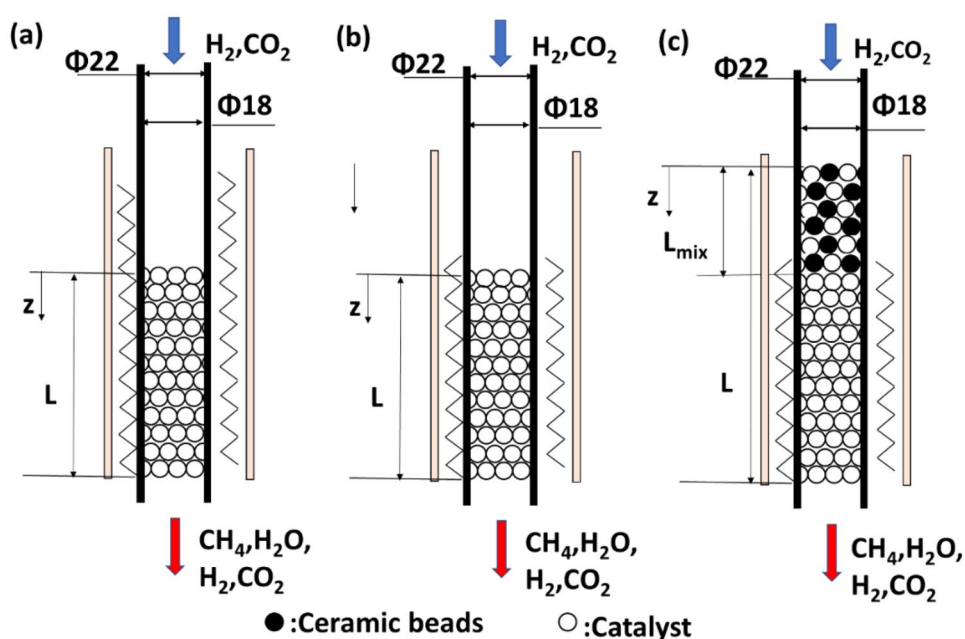


Table 1 Experimental condition

Case #	Experimental model (Fig. 5)	A_{cb}/A_{cat}	Catalyst weight in mixing layer, g	L (L_{mix}), mm	Space velocity, 1/h
S	(a)	—	—	40 (0)	5900
S'	(b)	—	—	40 (0)	5900
1	(c)	1	1	35 (10)	5200
2	(c)	4	1	35 (25)	3900

A_{cb} and A_{cat} : Surface area of ceramic beads and catalyst

has cylinder-shape (3.2 mm diameter and 3.2 mm height). The total amount of catalyst in the reactor is 8 g and filled in the reactor as shown in Fig. 5. The following three series of the reactor design to manage the heat release as well as the heat dissipation are considered in this study. In (a), no additional layer in the upstream of the standard catalyst layer (case S) and full-of-cylinder is heated by heater. By this way, the incoming gas is well-preheated. In (b), heating regime is limited to the location where the catalyst is packed (case S'). In (c), an additional layer formed in the upstream to impose “non-uniform (stepwise) distribution of catalyst” by mixing with chemically-inert ceramic spherical beads (Al_2O_3), whose diameter is 3 mm. Note that the heater arrangement is exactly the same as (b). Mixed ratio of catalyst to the ceramic beads is varied from 50% (case 1; diluted in half) and 80% (case 2: highly-diluted) by exposed surface area, respectively. Table 1 summarizes the experimental conditions applied in this work, where A denotes approximate surface area and subscript of cb and cat represent ceramic beads and catalyst, respectively.

2.3 Temperature Measurement

In this study, we employ two ways to monitor the temperature distribution inside the reactor. One is the fixed location pattern for checking the time-sequence temperature measurement (Fig. 6). Five K-type sheath TCs (Type K-316-1.6; surrounded by SUS 316 and 1.6 mm of its outer diameter) are bundled at various length and inserted from the downstream through the sealed connector. Location of TCs are A: 2 mm, B: 11 mm, C: 20 mm, D: 29 mm, and E: 38 mm, respectively, from the top-end of the catalyst layer. The other is for measurement of steady-state temperature profile by moving TC from the upstream to the downstream.

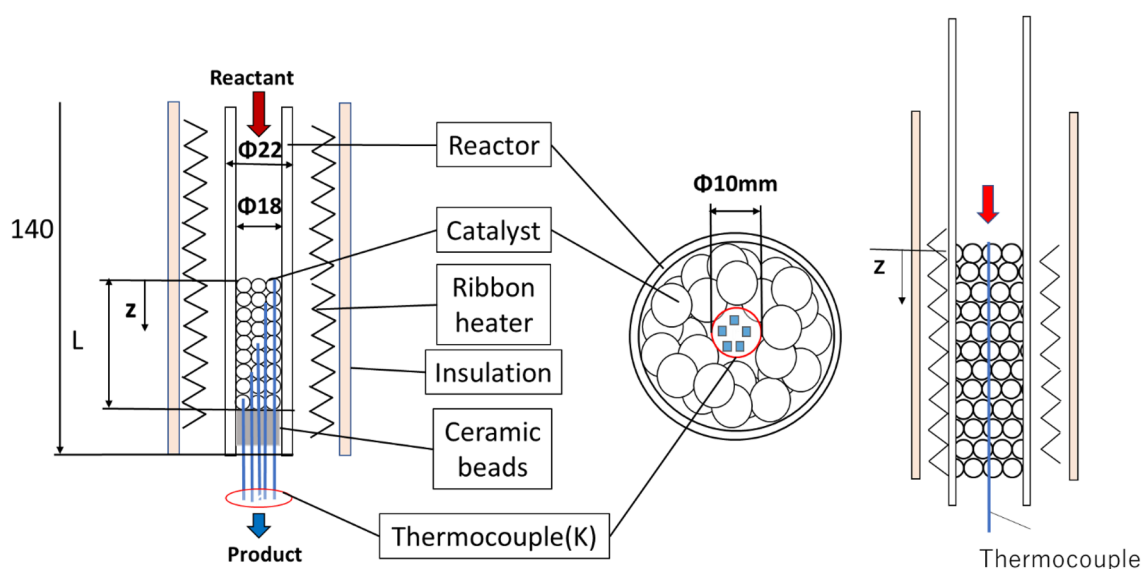


Fig. 6 Thermocouple location in the reactor (for case S); left five-TCs' arrangement for time-sequence temperature measurement, right: movable single TC for steady-state temperature profile measurement

3 Experimental Results and Discussion

3.1 For Case S (Standard Configuration)

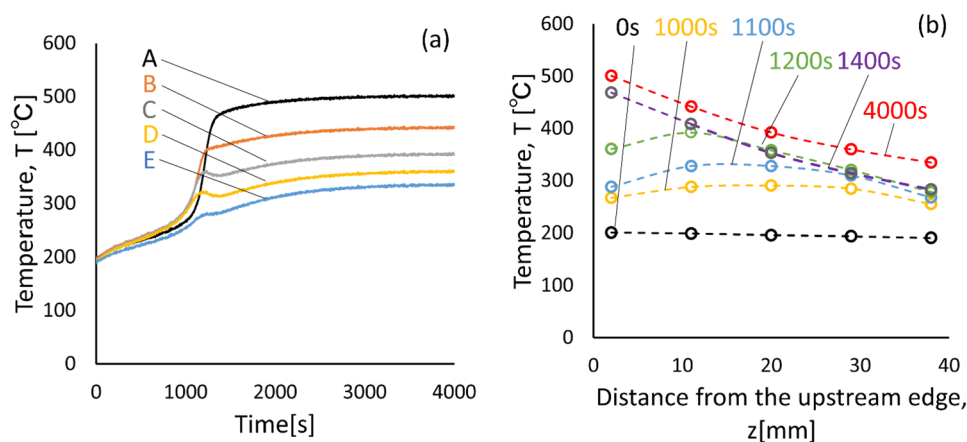
3.1.1 How to Reach the Steady-State

Firstly, we shall present how to achieve the steady-state in the present reaction system in case S as representative example. In Fig. 7, time-variation of temperature signal recorded by the five mounted TCs (A-E) are shown. Time zero is defined as the moment of the reactant gas is flowing into the preheated reactor at the prescribed temperature (250 °C in the present representative case).

As indicated in Fig. 7a, the reactant gas mixture gradually is heated up in the reactor, and sharp increase of temperature is found after 1000 s, suggesting that the ignition

is experienced. Interestingly, the peak temperature history is found only at location C and D (20 mm and 29 mm from the upstream edge, respectively), denoting that the ignition occurs around here. Once the ignition is taken place in the middle of the reactor, thermal wave travels to upstream where the fresh mixture is expected to promote the increase the local temperature there, then eventually the very close to the inlet (location A: 2 mm from the upstream edge) reach the maximum value around 1200 s. This process seems similar to the upward flame propagation although there is no flame is presented (we only have exothermic front instead). After 1200 s, temperature variation in time becomes gentle at all TCs and eventually approaches towards constant value, suggesting that the steady-state is achieved. Figure 7b is replotted of Fig. 7a in a different fashion showing the variation of temperature

Fig. 7 Time variation of five-TCs signals embedded in the reactor for case S, **a** time vs temperature, **b** position vs temperature



profile in time. Throughout this study, the steady-state is considered when $dT/dt < 0.0033 \text{ K/s}$ (less than $1.0 \text{ }^\circ\text{C}$ per 5 min) is satisfied (noted that, although not shown here, in the preliminary test, temperature stays constant even over 4000 s).

3.1.2 Conversion Performance at Steady-State

In Fig. 8, conversion performance is summarized by the maximum temperature found at the upstream edge (for case S). Variation of the maximum temperature can be obtained by various preheating conditions. This figure clearly shows the fact that the conversion rate can reach nearly 80% for higher temperature condition ($> 400 \text{ }^\circ\text{C}$). Because the conversion rate is levelling off over $450 \text{ }^\circ\text{C}$, we could confirm that the too-high temperature is not always good. It is suspected that CO production would be more pronounced under such condition. Although not shown in this figure, we have confirmed that this trend is quite consistent even at different reactant flowrate is imposed or the catalyst layer length is varied.

3.2 For Case S': Limited Preheating Length (Only at the Catalyst Bed)

For case S, because the incoming gas mixture is also preheated sufficiently, exothermic reaction suddenly occurs when the gas meets the catalyst (namely, the upstream edge of the catalyst). To prevent such temperature spike, preheating zone is limited to the catalytic bed and incoming gas is kept low temperature when it is loaded into the catalyst layer (case S'). In this way, we could avoid the immediate

exothermic reaction at the upstream edge and shift the reactive zone to downstream. This may promote the heat loss from the reactive zone to both (upstream and downstream) directions via conduction and radiation.

Typical temperature profile at the steady-state is shown in Fig. 9. It is clearly notified that the sharp temperature spike at the upstream edge for case S (see Fig. 7) is successfully suppressed, instead, the peak moves toward 10 mm downstream from the edge as expected. However, the peak temperature is not reduced drastically even though the heat loss toward the upstream through the catalyst shall be promoted, probably because of the heat recirculation effect often appeared in combustion system in the porous medium [20]. A peak shift contributes to the expansion of the regime over $400 \text{ }^\circ\text{C}$ at which the higher conversion is expected, resulting that the total conversion performance is improved as compared to Table 1. However, the increment is limited to only several percentage (Table 2).

According to the previous work using homogeneous reactor [1], the maximum conversion ratio ($\sim 80\%$) achieved at equilibrium state is matched over $450 \text{ }^\circ\text{C}$ for $\text{Ru}/\text{Al}_2\text{O}_3$ catalyst. Interestingly this trend is quantitatively matched to the present study (Fig. 8), even though Fig. 8 is evaluated with “maximum” temperature. This fact implies that the maximum temperature in this study for case S (or S'),

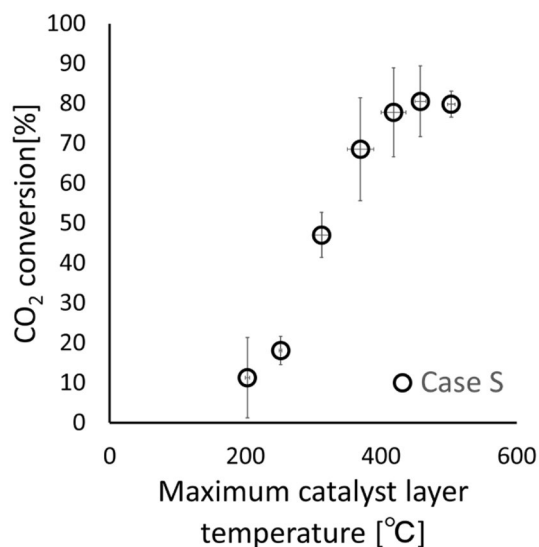


Fig. 8 CO_2 conversion rate depending on the achieved maximum temperature in the reactor (at upstream end) for case S

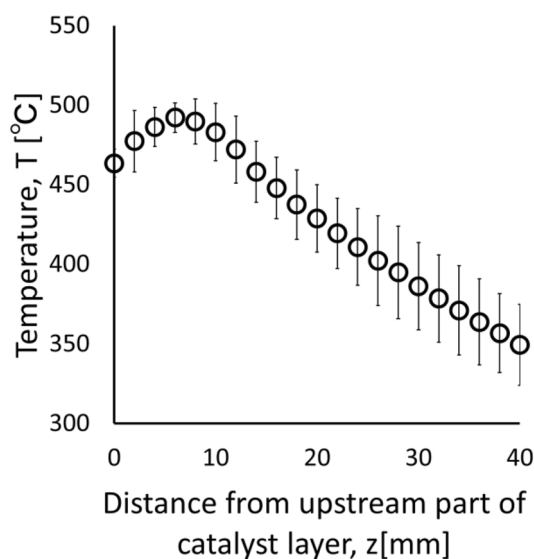


Fig. 9 1-D temperature profile for case S'

Table 2 Improvement of conversion performance by controlling the preheating zone

	CO ₂ conversion [%]
Case S	79.8
Case S'	82.4

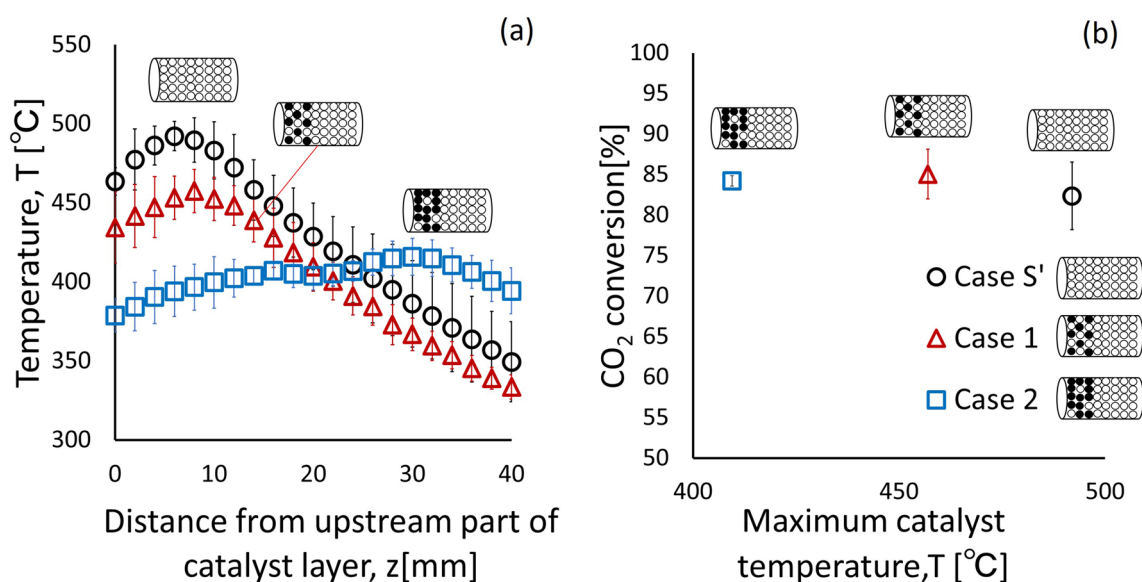


Fig. 10 Impact of the concept introducing non-uniform (stepwise) catalyst distribution, **a** temperature distribution along the axis, **b** CO₂ conversion performance

not the profile, can characterize the conversion performance of whole reactor; in other word, the fast conversion might be attained only around the location showing the temperature peak and immediately the system reaches to the equilibrium state. This is consistent to the observed fact that the reactor length is rarely affected on the conversion performance as described in Sect. 3.1.2.

This brings us idea of two choices for the reactor design; one is to make very short reactor to form the hot spot there over 450 °C to promote the equilibrium state there and the other is longer reactor to have slower conversion in wide zone. Former seems fine, however, the conversion rate cannot exceed 80% which is upper limit determined by the chemical equilibrium and CO might be produced and the catalyst may be subjected to the thermal damage. In this sense, this choice is easy but not be recommended. Consequently, we shall take the latter choice; namely, conversion (reactive) zone must be spread out the wide portion of the reactor and reduce the whole reaction temperature. When it is reduced less than 420 °C, CO production shall be suppressed and the thermal damage can be avoided.

3.3 Impact of the Non-uniform (Mixing) Catalyst Distribution Concept

Recall that the key issue here is to achieve lower maximum temperature (< 450 °C) in the reactor and over activated temperature for conversion (> 250 °C). Suppose we could achieve nearly “flat” temperature profile less than 400 °C, all requirements are fulfilled. In order to spread the reactive zone all over the reactor, we attempt to introduce

“non-uniform catalyst distribution” concept. Taking advantage of the catalytic reaction system, we shall control the heat release rate and conversion performance by managing the concentration of the catalyst over the substrate. Imagine that we have very “lean” catalyst in the reactor, even we have reactant flowing over it, complete conversion cannot be made, accordingly, hot spot formation is effectively suppressed. However, reaction rate is not fast enough so that the unreacted gas is remained. Thus, if we have two zones structure of the catalytic layer (lean catalyst zone followed by the rich catalyst zone; called “stepwise catalyst distribution”), we may expect to form the “less peak structure” in the temperature distribution and conversion reaction may occur in wide location in the reactor, then the unreacted gas is not remained much. As example, we attempt to introduce two cases (case 1 and 2), placing the diluted catalyst layer ahead of the upstream edge of the uniformed catalyst layer. Each case has different dilution pattern to test the effectiveness of the present approach.

Figure 10 shows the temperature distribution and the CO₂ conversion rate for the tested cases 1 and 2. It is found that having the stepwise catalyst distribution results in the decrease of maximum temperature and its peak location moves to downstream. Most importantly, it is successfully achieved the flat temperature profile (see case 2). From the temperature distribution, it is suspected that the reactive zone shall be widely distributed inside the reactor. Although the local reaction rate stays slower due to lower temperature, the wider reactive zone may compensate to maintain the conversion rate satisfactory as shown in Fig. 10b. For the both case S' and case 1, unreacted CO₂ is hard to be converted

since the temperature at the outlet is too low and the reaction status is close to be frozen. For case 2, on the contrary, outlet temperature is still high enough so that the further reactivity could be expected when the additional catalyst zone is added. Hence when the longer reactor is employed at downstream, unreacted CO₂ has chance to be reacted and achieving a higher conversion rate might be expected.

To end, the new arrangement based on “controlling catalyst distribution profile” can bring at least two merits: (1) we could successfully avoid to appear the local hot spot (concentrated reactive zone) to improve the durability of the system (by avoiding thermal damage of the catalyst) and the stability to avoid any potential thermal runaway, (2) not only a part of catalyst but whole catalyst in the reactor to participate the conversion (this is most efficient way to utilize the catalytic activity).

4 Concluding Remarks

A novel engineering concept to introduce the stepwise catalyst distribution is proposed and tested in order to achieve less-peak reactor temperature distribution in tube-type of Sabatier reactor. This brings at least two merits in terms of durability as well as stability; one is to avoid to appear “hot spot” in the reactor to improve the durability and the other is to achieve high conversion performance by participating wide-range of low temperature catalytic layer. Our experimental results conformed the effectiveness of the presently proposed concept. With the present approach, due to achievement of near-flat temperature profile, the outlet of catalyst bed could be maintained at relatively high temperature. Hence employing additional catalyst zone at downstream can convert unreacted CO₂ to deliver higher conversion performance.

Acknowledgements Technical advices and fruitful discussions brought by Drs. Shima and Sakurai from JAXA, are very much appreciated. Assistance provided by Ms. Tomita from TUT for providing GC data is greatly helpful.

Compliance with Ethical Standards

Conflict of interest All authors have no conflict of interest.

Affiliations

Shinya Sakamoto¹ · Tsuneyoshi Matsuoka¹  · Yuji Nakamura¹ 

✉ Yuji Nakamura
yuji@me.tut.ac.jp

References

1. Tada S, Ochieng OJ, Kikuchi R, Haneda T, Kameyama H (2014) *Int J Hydrog Energy* 39:10090–10100
2. Marocco P, Morosanu EA, Giglio E, Ferrero D, Mebrahtu C, Lanzini A, Abate S, Bensaid S, Perathoner S, Santarelli M, Pirone R, Centi G (2018) *Fuel* 225:230–242
3. Kok E, Scott J, Cant N, Trimm D (2011) *Catal Today* 164:297–301
4. Gonzalez LM, Vries DC, Claeys M, Schaub G (2015) *Catal Today* 242:184–192
5. Bossel U, Eliasson B (2003) *Energy and the hydrogen economy*. ABB Switzerland Ltd, Oberrohrdorf
6. Müller K, Fleige M, Rachow F, Schmeiber D (2013) *Energy Procedia* 40:240–248
7. Anderson MS, Ewert MK, Keener JF, Wagner SA (2015) *Life support baseline values and assumptions document*. National Aeronautics and Space Administration, Washington, DC
8. Aeronautics N, Administration S (2018) *National space exploration campaign report*. National Aeronautics and Space Administration, Washington, DC
9. Drake BG (2009) *Human exploration of mars design reference architecture 50 addendum*. National Aeronautics and Space Administration, Washington, DC
10. Shima A, Sakurai M, Sone Y, Ohnishi M, Yoneda A, Abe T (2018) In: *Proceedings of the Japan society for aeronautical and space sciences JSASS-2018-4494* (in Japanese)
11. Samplatsky DJ, Grohs K (2011) In: *Proceedings of the 41st international conference on environmental systems AIAA-2011-5151*
12. Miyakoshi A (2015) JP6209398B2. Japan Patent Office, Tokyo (**in Japanese**)
13. Greenwood ZW, Abney MB, Wall T (2017) In: *Proceedings of the 47th international conference on environmental systems ICES-2017-182*
14. Sakai Y, Tachihara S, Oka T, Waseda S, Sakurai M, Shima A, Nakanoya S (2018) In: *Proceedings of the 62st space sciences and technology conference JSASS-2018-4493* (in Japanese)
15. Rostrup-Nielsen JR, Pedersen K, Sehested J (2007) *Appl Catal A-Gen* 330:134–138
16. Bartholomew CH (2001) *Appl Catal A-Gen* 212:17–60
17. Kiewidt L, Thöming J (2015) *Chem Eng Sci* 132:59–71
18. Brooks KP, Hu J, Zhu H, Kee RJ (2007) *Chem Eng Sci* 62:1161–1170
19. Sun D, Khan FM, Simakov DSA (2017) *Chem Eng J* 329:165–177
20. Takeno T, Sato K (1979) *Combust Sci Technol* 20:73–84

Publisher's Note Springer Nature remains neutral with regard to jurisdictional claims in published maps and institutional affiliations.

¹ Department of Mechanical Engineering, Toyohashi University of Technology, 1-1 Hibarigaoka, Tempaku, Toyohashi 441-8580, Japan